\Asian Journal of Chemistry Vol. 19, No. 1 (2007), 175–186

Effective Parameters in Computational Fluid Dynamics Simulation of Baffled Stirred Column Reactor Hydrodynamics with Sliding Mesh

R. RAHIMI, M. ZIVDAR, M.A. SALEHI*, F. SHAHRAKI and H. GHANNADZADEH†

Department of Chemical Engineering, Sistan and Baluchestan University Shahid Nikbakht Faculty of Engineering, Daneshgah A.V., Zehedan, Iran
E-mail: salehi@hamoon.usb.ac.ir

The main objective of this research is to investigate a mathematical model for use in simulations of baffled stirred reactor hydrodynamics. To evaluate this model, simulations are done for a single-phase impeller stirred vessel in the laboratory. These results are then compared with experimental data from literature. For the single phase system, two different turbulence models were tested. It is clear that the modified model of Chen and Kim for impeller stirred systems is far superior to the standard model used for bubble stirred systems. Also a comparison of sliding mesh, snapshot and empirical source models for impellers are done for the same system. It is shown that the sliding mesh model and the snapshot model give similar results, which may be a small preference for the sliding mesh model. The empirical source model is believed to give good results on time average.

Key Words Computational fluid dynamics, Baffled stirred reactor, Sliding mesh hydrodynamics, Mathematical effective parameters.

INTRODUCTION

For thousands of years man has used the fermentative abilities of micro-organisms. Brewing has been done for at least 8000 years and yeast-production for about 6000 years. In modern times the commercial use of fermentation has been rapidly growing, particularly due to the need for pharmaceutical products, and in food industry. The modern accepted bioreactor or fermenter, which is a stirred tank, was developed in the 1940s. This development was accelerated because of the large demand for antibiotics during the Second World War. Not all bioreactors are stirred tanks. In fact, most reactors are non-stirred and may also be non-aerated with their use in wastewater treatment and wine, beer and yoghurt production. However, high value products like antibiotics are all produced in stirred reactors.

†Department of Chemical Engineering, Guilan University, Rasht, Iran.

Simulations of flow in single-phase stirred vessels have been performed. The single-phase vessel has been simulated to verify the impeller models and the turbulence models for swirling systems. Based on these verifications, the models used for the two-phase vessel and the fermenter are chosen. Ranade *et al.*[1-3] have done extensive LDA measurements of the flow generated by a Rushton turbine in a baffled vessel. These data are used for verifications of the CFD code. Fig. 1 gives a schematic diagram of the vessel. The impeller is a standard six-bladed Rushton turbine. There are four baffles with no gap between the baffles and the wall. Tap water at ambient temperature and pressure was used as fluid, and the impeller speed chosen was 300 rpm. Fig. 2 gives the numerical grid used for the simulation. The calculation domain is discretized by a mesh of (17 ×40 × 26) grid nodes in the radial, tangential and axial direction, respectively. The top of the

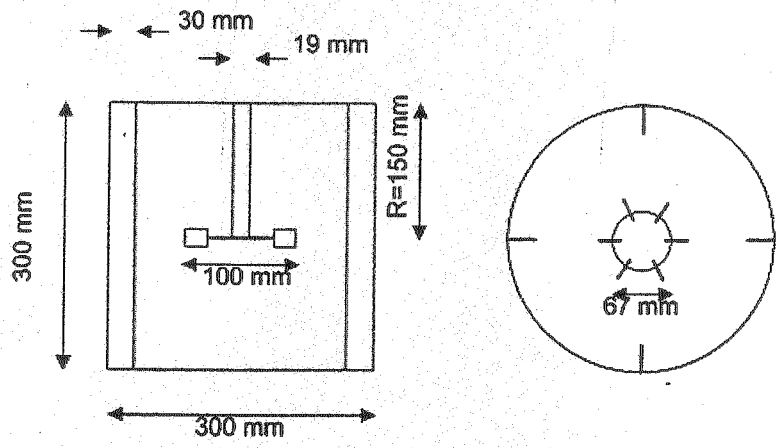

Fig. 1 Schematic diagram of the vessel

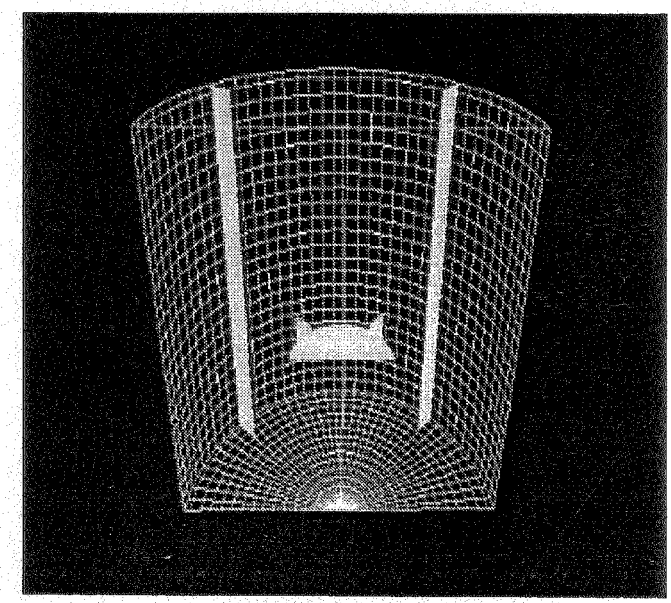

Fig. 2. Numerical grid used for the simulation (six-bladed Rushton turbine and four baffles with no gap between the baffles and the wall)

reactor is assumed to be open to the atmosphere and therefore regarded as a free, fiat surface (free-slip).

Theory: In the case of baffled tanks, the simulation of non-moving baffles and rotating impeller blades is not an easy task. The common approach until a few years ago has been to do either some kind of stationary simulations or by representing the action by using distributed sources of momentum. During the last years the rapid development of high-performance computers has made the development of more sophisticated models possible. Two of the more advanced approaches are to use moving deforming mesh techniques or to use a sliding mesh. The former needs much bookkeeping and may lose accuracy during deformation. The latter method is much easier to implement and is standard in many commercial codes. The sliding mesh technique is therefore chosen in this paper. For a comparison also a distributed source method and a snapshot method have been tested. This comparison is presented in the figures. A comparison of the sliding mesh technique and the snapshot approach has also been done by Harvey and Rogers[2], but only for a laminar case.

Mathematical model: The mathematical models given are discretized by the finite volume method. The computational domain is divided into a finite number of non-overlapping control volumes in a three-dimensional cylindrical coordinate system as shown in Fig. 3 (a). The sizes of the control volumes can differ

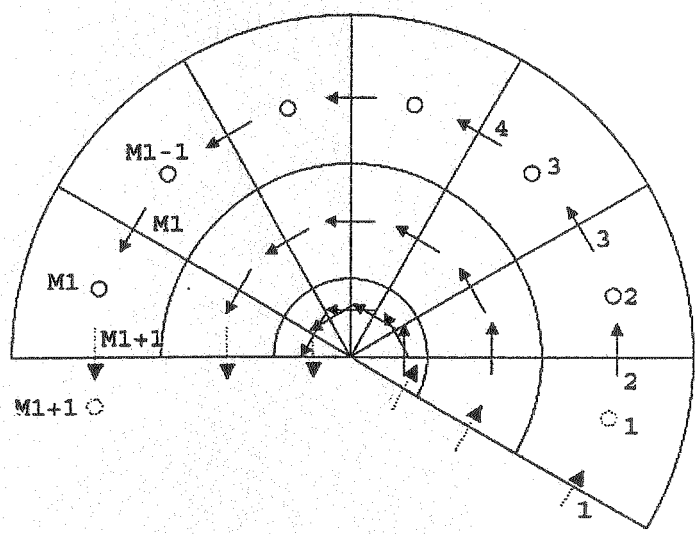

Fig. 3. (a) Grid used for periodic boundaries (dotted arrows are velocities in fictitious points)

independently along each co-ordinate direction. In the centre of each control volume, a main node is placed for which all scalar variables are solved and stored. The values of the variables are assumed to be uniform in each control volume. A staggered grid arrangement is adopted for the velocity components, which are stored at the surfaces of the main control volumes. The staggered grid arrangement is introduced to avoid an alternating, unphysical pressure field that will be felt like a uniform pressure field by the momentum equations. The staggered grid arrangement is shown in Fig. 3 (c).

The model is based upon the Eulerian model originally derived by Ishii[6] and

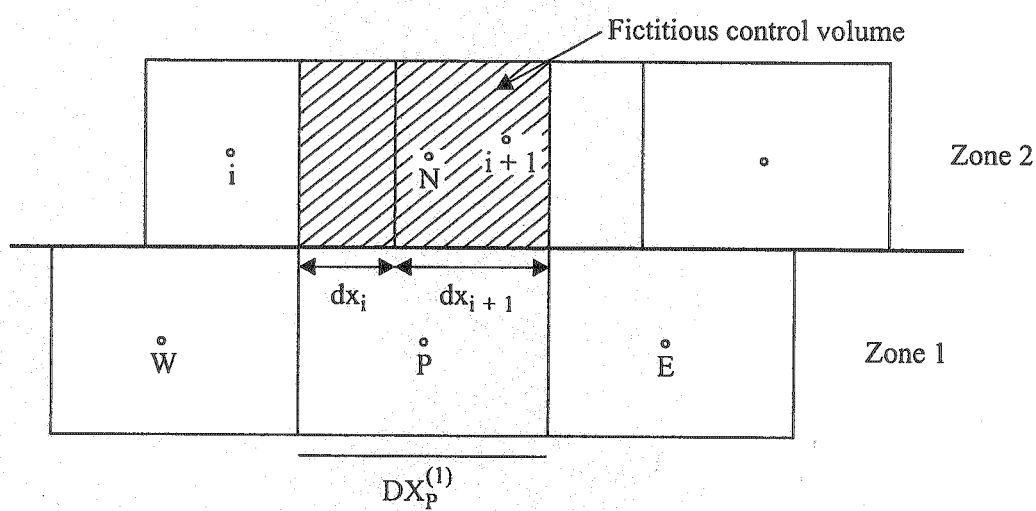

Fig. 3. (b) An interfacial interpolation for flow variables and fluxes across the sliding surface

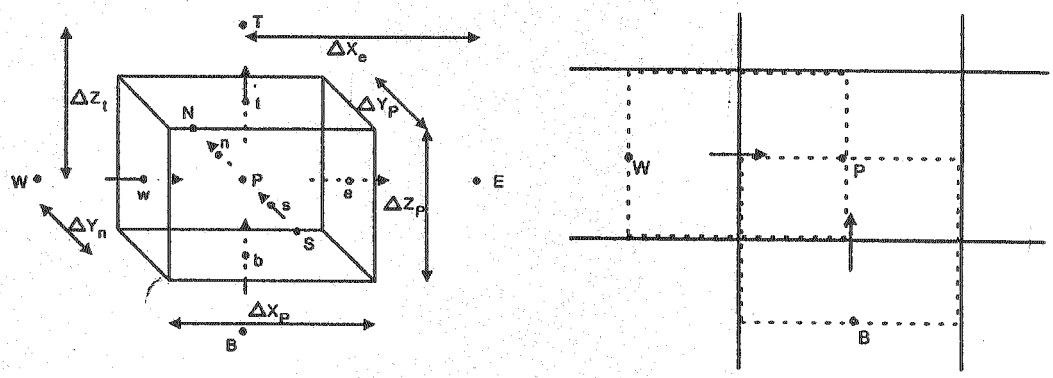

Fig. 3. (c) 3-dimensional control volume for scalar variables and 2-dimensional control volume for velocities

later improved by Spalding[7] and Drew[8, 9] among others. There is a general acceptance for the exact equations of motion to be written as:

$$\frac{\partial \rho\phi}{\partial t} + \frac{\partial}{\partial x_i} \rho\phi v_i = \frac{\partial}{\partial x_i} J + \rho f \qquad (1)$$

TABLE-1
VARIABLES USED IN THE GENERAL CONSERVATION EQUATION

	ϕ	J	f
Mass	1	0	0
Momentum	$\vec{v}$	$-PI_{ij} + \tau_{ij}$	g

This equation is exact inside each phase and can at least in theory be solved exactly for simple cases. At an interface between the phases, properties are discontinuous, although mass and momentum must be conserved. If accumulation terms are neglected, Ishii[6] gives the jump conditions valid across the interface:

$$[(\rho\phi(\vec{v} - \vec{v}_{interface}) + J) \cdot n] = M_{interface} \qquad (2)$$

where the value for interface is 0 for mass conservation. It is also 0 for momentum conservation when no reaction appears and the surface tension is constant. A further discussion on this term may be found in for instant Ishii[6] and Drew[8]. Since eqn. (2) is derived using integral balances, these discontinuities cause mathematical problems. Except for some very simple cases this set of equations are impossible to solve on computers of today. It is therefore a need for some kind of averaging technique for the equations to find a representation that is possible to solve. Several different techniques are used, with volume averaging, time averaging and ensemble averaging as the three most important ones. The first two may be seen as simplified versions of the latter. They all result in very similar equations. The small differences are only of philosophic interest since they all give terms that have to be further modelled, and then of course are not exact. Therefore the conservation equations used in computational fluid dynamics (CFD) society are more or less the same regardless of what averaging technique is used. There are however some important exceptions resulting from different interpretations of the rules for averaging. In this research, the time-averaged equations given by Ishii[6] are used. However, other investigators using ensemble averaging develop some models used for interfacial forces. After averaging the general transport equations, we get the following set of multi-phase conservation equations:

Mass:

$$\frac{\partial}{\partial t}(\beta_V \alpha_k \rho_k) + \frac{\partial}{\partial x_i}(\beta_i \alpha_k \rho_k v_{i,k}) = 0 \tag{3}$$

Momentum:

$$\frac{\partial}{\partial t}(\beta_V \alpha_k \rho_k v_{j,k}) + \frac{\partial}{\partial x_i}(\beta_i \alpha_k \rho_k v_{i,k} v_{j,k}) = -\beta_V \alpha_k \frac{\partial P}{\partial x_j} - \frac{\partial}{\partial x_i}(\beta_i \alpha_k \tau_{ij,k}) + \beta_V \alpha_k \rho_k g_j + M_{i,k} \tag{4}$$

Scalar:

$$\frac{\partial}{\partial t}(\beta_V \alpha_k \rho_k \phi_k) + \frac{\partial}{\partial x_i}(\beta_i \alpha_k \rho_k v_{i,k} \phi_k) = -\frac{\partial}{\partial x_i}(\beta_i \alpha_k J_{\phi,k} + S_{\phi,k}) \tag{5}$$

The global mass conservation is given by:

$$\sum_{k=1}^{n} \alpha_k = 1.0 \tag{6}$$

Here the subscript k refers to the phase k, i.e., gas (g) or liquid (l), and may be any of the transported scalar variables. Three terms from these equations have to be modelled: shear stresses, $\tau_{ij,k}$, turbulent diffusive transport of scalar variable, $J_{\phi,k}$ and interfacial momentum transfer, $M_{i,k}$. $M_{i,k}$ will be described later and are related to the mean flow field through the Boussinesq approximation[10–12] and are given by the following expressions:

$$\tau_{ij,k} = \mu_{i,k}\left[\left(\frac{\partial v_{j,k}}{\partial x_i} + \frac{\partial v_{i,k}}{\partial x_j}\right) - \frac{2}{3}\delta_{i,j}\frac{\partial v_{m,k}}{\partial x_m}\right] \tag{7a}$$

$$J_{\phi,k} = -\frac{\mu_{t,k}}{\sigma_\phi}\frac{\partial_{\phi k}}{\partial x_i} \tag{7b}$$

Interfacial forces: The interfacial coupling term, M_k, is a linear combination of several underlying forces. This is given by the following expression:

$$M_k = M_k^D + M_k^P + M_k^{VM} + M_k^L + M_k^W + M_k^{WF} + M_k^{TD} \tag{8}$$

where D = interfacial drag force, P = interfacial pressure coupling terms that arise due to the pressure differences across liquid interfaces, VM = virtual mass (or added mass) force, L = lift forces, W = lubrication force which is a wall law for the gas, WF = drag force that the wall exerts on the bubbles and TD = correction for the effects of non-linearity in the other forces.

Sliding mesh

The basic idea is to employ two grids: one moving with the impeller while the other fixed to the tank walls. The two meshes interact along a common surface. The moving grid is allowed to slide relative to the stationary one and grid lines are not required to align on the common surface. This makes it possible to have an exact model for the impellers and the baffles. An example is shown in Fig. 1. An interpolation routine is used to obtain flow variables and fluxes across the sliding surface.

$$\phi_P^{(1)} = \frac{\left(\phi_i^{(2)} dx_i^{(2)} + \phi_{i+1}^{(2)} dx_{i+1}^{(2)}\right)}{DX_P^{(1)}} \tag{9}$$

The basic methodology depends on the construction of fictitious meshes on both sides of the sliding interface. For a node P in Zone 1, the north neighbour is the fictitious node N. Similar fictitious neighbours are created for mesh points in Zone 2. The values of a variable in the fictitious points are obtained by linear interpolation. By using such an interpolation, the program is restricted to have uniform grid sizes in the tangential direction. The fictitious points are updated in the same manner as the regular points.

Snapshot method

The snapshot technique captures the flow characteristics of a stirred vessel at one time instant, using boundary conditions corresponding to that particular time instant[13]. The transient terms are neglected. When convergence has been achieved, the impellers are moved some degrees, and a new computation is started. The results from the different impeller positions are finally averaged. This approach seems only reasonable if the time dependent parts of the transport equations are negligible. To our knowledge, use of this method has only been reported for laminar cases. Since the flow is assumed to be steady state, the computational effort is less than that for the sliding mesh approach[14].

Comparison of turbulence models

It is known that the standard k-ε model is not well suited to describe swirling flow or internal recirculating flow problems[15, 16]. The modified model of Chen

and Kim[17] is therefore compared against the standard model to see if this model gives better predictions. For this comparison, the sliding mesh model is used for the impeller.

Radial velocity

Fig. 4 shows radial distribution of experimental and calculated radial velocities at distances of 30 mm above the impeller and 10 mm below the top of the vessel, respectively. As can be seen from the upper figure, the standard model seems to

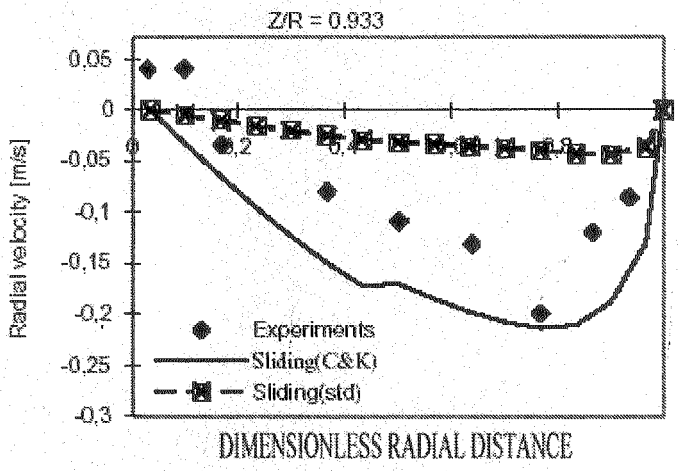

Fig. 4

give better predictions close to the impeller. On the other hand, the modified model seems to capture more of the radial dependence of the velocity, especially in the outer part. An interesting point is the relatively high experimental value close to the centre axis. This indicates that this system cannot be solved correctly with a model assuming axis-symmetry. Closer to the top the picture is very different, as can be seen in the lower plot. The standard model gives highly under predicted velocities, whereas the modified model has both the right shape and gives correct maximum velocity. This means that the model of Chen and Kim[17] predicts a much stronger recirculation above the impeller than the standard model. This is in accordance with the intention for the modification of the model. Again there is a problem predicting the velocities close to the centre axis[18].

Tangential velocity

Fig. 5 shows tangential velocities 30 mm above the impeller and 10 mm below the top of the vessel, respectively. Here, the standard model is completely wrong at both heights. The modified model, on the other hand, gives good predictions close to the impeller level, especially in the outer region. Closer to the top the predictions are not good, but still better than the standard model. As for the radial velocities it is impossible to predict velocities at the centre axis when axis-symmetry is assumed. The discrepancy close to the top may be explained with lack of knowledge of the real boundary conditions, which probably is not a fiat, free surface.

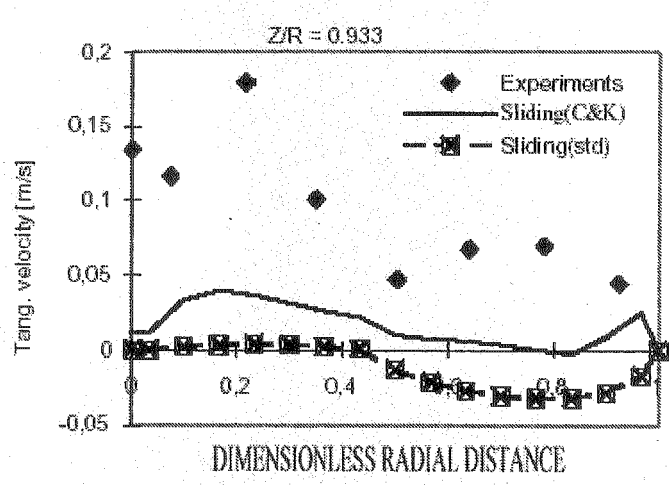

Fig. 5

Axial velocity

Experimental values of axial velocities are reported at four different heights and are compared with the simulations in Fig. 6. It can be seen that the modified model gives very good predictions for all four levels. Only the top level could be somewhat better predicted. Again, this may be explained with the use of a free, fiat surface as a boundary condition. The standard model strongly under predicts the velocities at all levels, but the directions seem to be correctly predicted.

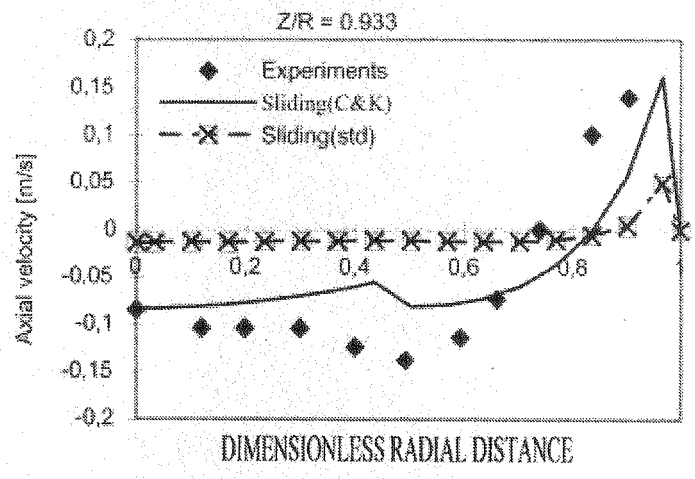

Fig. 6

Turbulent kinetic energy

Experimental data for the turbulent kinetic energy is only given at the level halfway between the impeller and the top. A comparison against the simulations is given in Fig. 7. It can be seen that the modified model gives surprisingly good agreement with the experimental data. The standard model gives on the other hand large over predictions. The shape of the profile is not good either. It is clear that the modified model gives far better predictions for all velocities and turbulent kinetic energy. Therefore this model is chosen for all simulations of impeller stirred vessels. For bubble columns the standard model is of course still used.

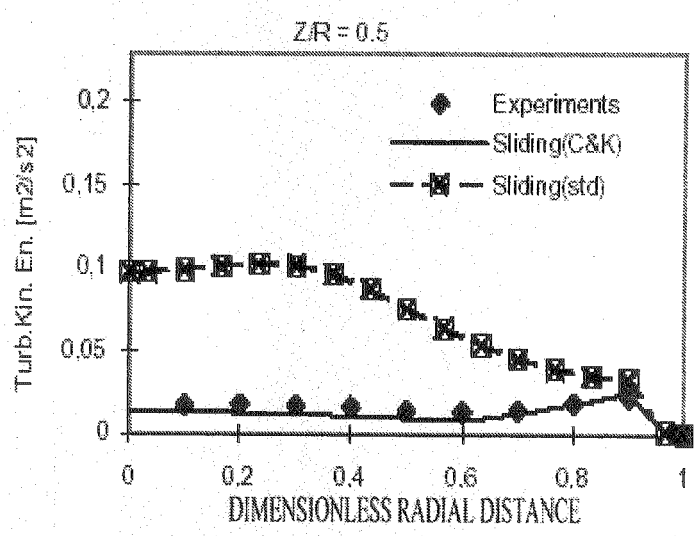

Fig. 7

Comparison of impeller models

The empirical source model, the snapshot model and the sliding mesh model will be compared. For the snapshot model, computations are done for seven equally spaced angles between impeller blades and baffles. These computations are then averaged. Radial velocity (Fig. 8) gives a comparison of computed radial velocity using sliding mesh, snapshot and an empirical source, respectively. All models give the same shape for the profiles both close to the impeller, and close to the top. Especially the snapshot and the sliding mesh models give very similar results. In both positions the empirical model predicts smaller values than the other two models. This under prediction of the recirculating flow is significant in the upper part.

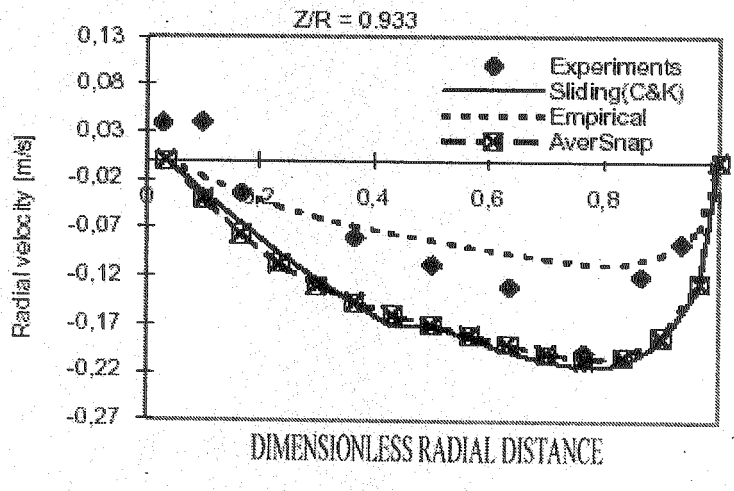

Fig. 8

Tangential velocity

Also for the tangential velocity, the results for the sliding mesh and the snapshot models are very similar close to the impeller level, as can be seen in Fig. 9. The only significant difference is the better predictions of the sliding mesh

model close to the symmetry axis. The predictions of the empirical model follow the results of the snapshot method, except in the wall region where the empirical model gives under predictions in the upper part of the tank. All models fail to predict the real values, but the sliding mesh model does predict the right direction of the flow. The other two models predict reversed flow in the tangential direction. The snapshot model and the empirical one give very similar results, with maybe the empirical model as a bit better than the snapshot model in this area.

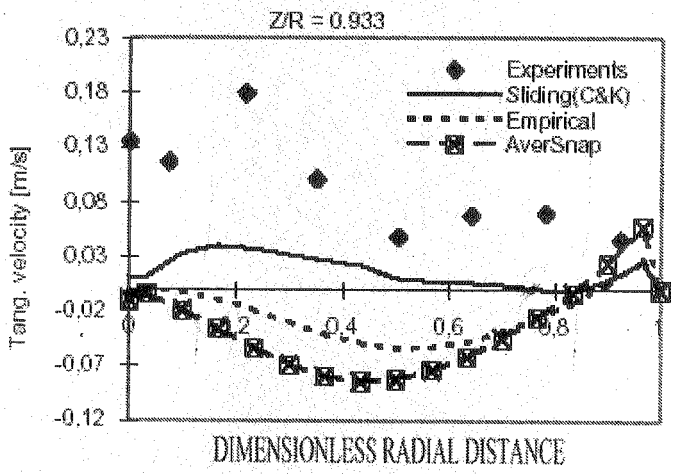

Fig. 9

Axial velocity

Fig. 10 shows that there are very little differences in the predictions of the sliding mesh model and the snapshot model for axial velocity. Both models give very good predictions at all levels. The empirical model gives the same shape of profiles as the other two models, but is under predicting at all levels.

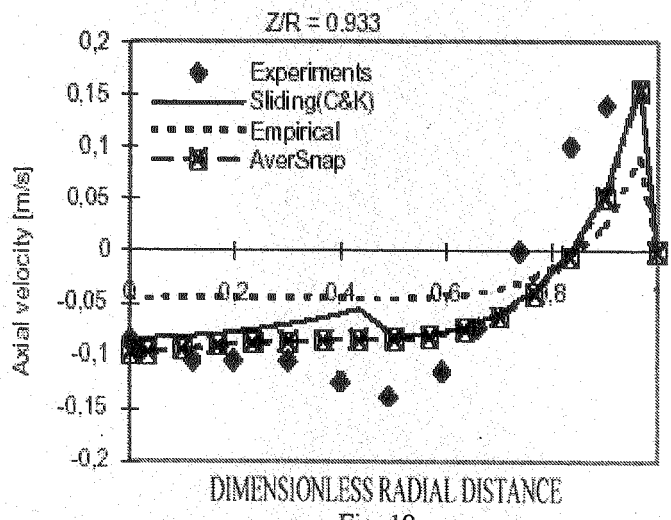

Fig. 10

Turbulent kinetic energy

As seen in Fig. 11, all three models give correct shape of the radial profile for turbulent kinetic energy. The snapshot models and the sliding mesh model are seen to be almost identical. These results are surprisingly good. The empirical

model gives slightly more under predictions than the other two, but also this result is relatively good. The results clearly show that the snapshot and the sliding mesh models give the best predictions. The sliding mesh approach is perhaps a little bit better than the snapshot approach. The choice between these two approaches has therefore to be taken on the basis of whether it is important to get details of the dynamics in the system and whether enough computational power is available to follow the sliding mesh approach. In this case, where ten iterations were used

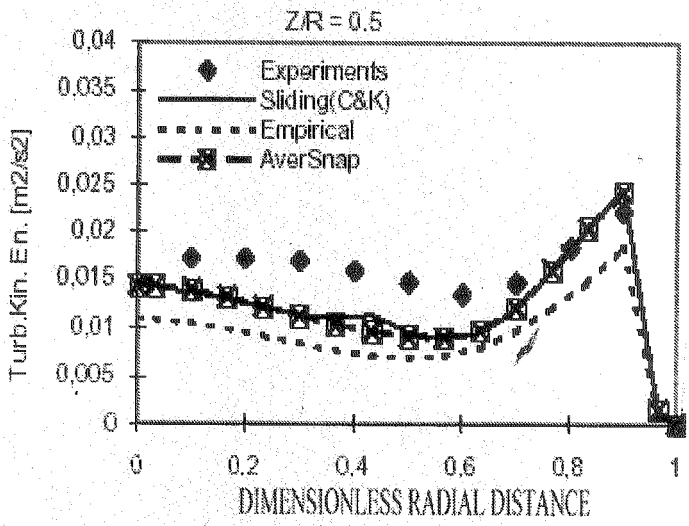

Fig. 11

for each time step, compared to seven averaged snapshots, there is no reason to prefer the snapshot method. For all cases the empirical model gives almost the same shape of profiles as the other two models, only more under predicted. This may be corrected for by tuning the drag coefficient; so this model may be a good choice for more complicated systems where the other two models are hard to implement.

Conclusion and recommendations

Therefore, using the best models the radial velocity is not too well simulated. The trends are correctly simulated, but the value is not correct. The tangential velocity is relatively well simulated close to the impeller, but not that well close to the top. This is probably because of wrong boundary setups for the upper boundary. The axial velocity is very well predicted in all parts of the vessel. In summary, the simulations of axial and tangential velocities are satisfying, whereas the simulations of radial velocities have less agreement with experiments. The simulation of turbulent kinetic energy is surprisingly well simulated using the model of Chen and Kim[17]. Only one set of experimental values, midway between the impeller and the top, is known. It is therefore not known if this good result is general for the whole vessel. But there is a need for tuning drag parameters. This model is probably a good alternative to more sophisticated models for more advanced impellers than the Rushton turbine. There is a need for experimental work to develop a model based on only known physiological parameters. The grid independency for the stirred column reactor should be examined.

REFERENCES

1. V.V. Ranade and H.E.A. vanden Akker, *Chem. Eng. Sci.*, **49**, 5175 (1994).
2. V.V. Ranade and J.B. Joshi, *Trans. I. Chem. E.*, **68A**, 19 (1990).
3. V.V. Ranade and J.B. Joshi, *Trans. I. Chem. E.*, **68A**, 34 (1990).
4. P.S. Harvey and M. Greaves, *Chem. Eng. Res. Des.*, **60**, 195 (1982).
5. A.D. Harvey III and S.E. Rogers, *AIChE J.*, **42**, 2701 (1996).
6. M. Ishii, Thermo-fluid Dynamic Theory of Two-phase Flow, Eyrolles, Paris (1975).
7. D.B. Spalding, in: R.W. Lewis (Ed.), Computer simulation of two-phase flows with special reference to nuclear reactor systems, Computational Technique in Heat Transfer, Pineridge Press, pp. 1–44 (1985).
8. D.A. Drew, *Ann. Rev. Fluid Mech.*, **15**, 261 (1983).
9. C. Hirsch, Numerical Computation of Internal and External Flows, Vol. I, John Wiley & Sons (1988).
10. M. Ishii and N. Zuber, *AIChE J.*, **25**, 843 (1979).
11. J.Y. Murthy, S.R. Mathur and D. Choudhury, CFD Simulation of Flows In Stirred Tank Reactors Using a Sliding Mesh Technique, ICHEME Symposium Series No. 136 (1994).
12. K.A. Pericleous and M.K. Patel, *Physicochem. Hydrodyn.*, **8**, 105 (1987).
13. A. Bakker and H.A.E. vanden Akker, *Chem. Eng. Res. Des.*, **72**, 583 (1993).
14. D.A. Drew and R.T. Lahey, *Int. J. Multiphase Flow*, **13**, 113 (1987).
15. C.Y. Perng and J.Y. Murthy, *AIChE Symposium Series*, **89**, 37 (1993).
16. I. Rousar and H.E.A. vanden Akker, LDA measurements of liquid velocities in sponged agitated tanks with single and multiple Rushton turbines, ICHEME Symposium Series, No. 136 (1994).
17. Y.S. Chen and S.W. Kim, Computation of turbulent flows using an extended k-ε turbulence closure model, Technical Report, NASA Contractor Report (1987).
18. T.H. Cook and F.H. Harlow, *Int. J. Multiphase Flow*, **12**, 35 (1986).

(*Received*: 25 July 2005; *Accepted*: 29 May 2006) AJC-4923